Organoid cystogenesis reveals a critical role of microenvironment in human polycystic kidney disease

Supplemental Information (7 figures and 4 movies)

Nelly M. Cruz, Xuewen Song, Stefan M. Czerniecki, Ramila E. Gulieva, Angela J. Churchill, Yong Kyun Kim, Kosuke Winston, Linh M. Tran, Marco A. Diaz, Hongxia Fu, Laura S. Finn, York Pei, Jonathan Himmelfarb, Benjamin S. Freedman

Supplementary Figure 1

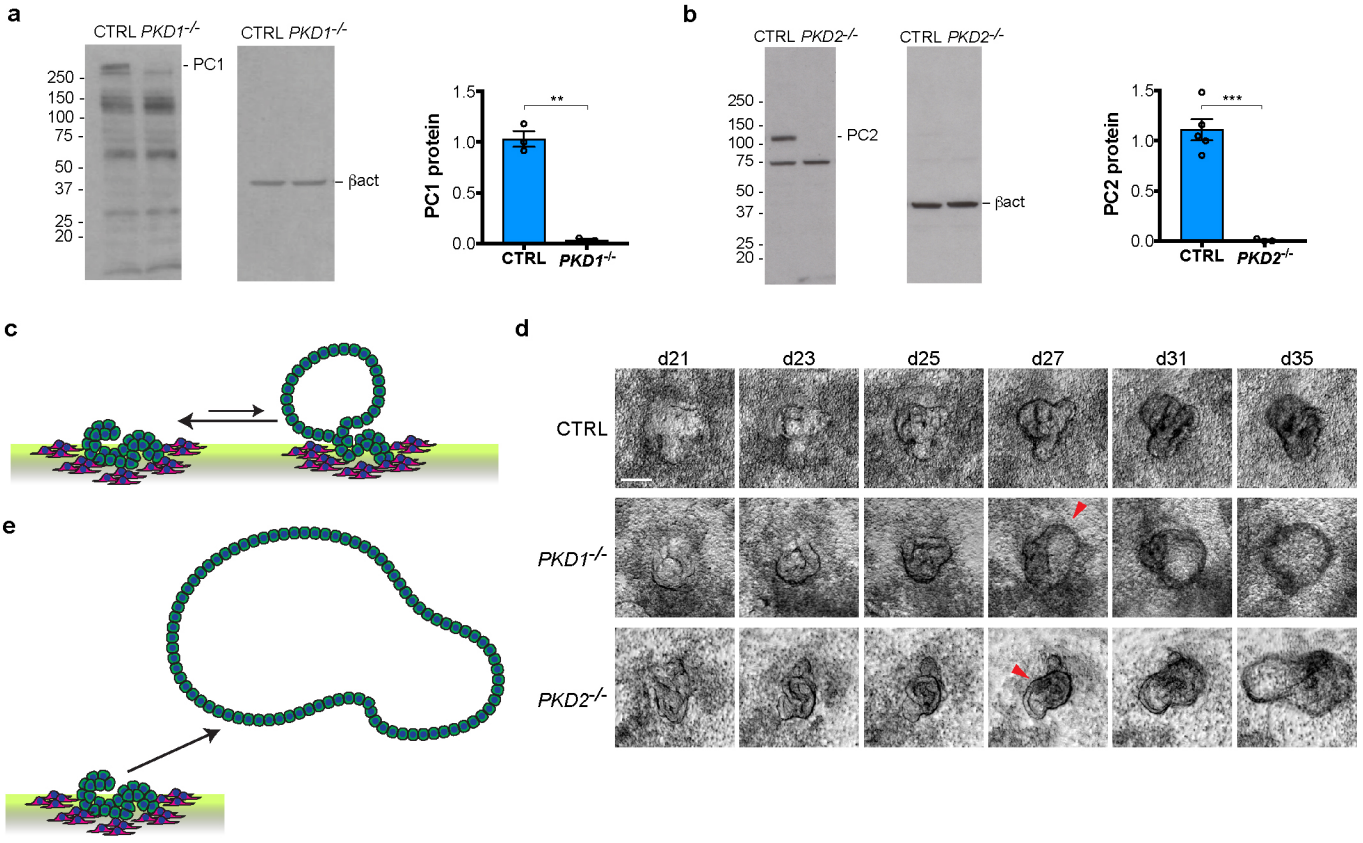

Supplementary Fig. 1. Analysis of adherent PKD organoids reveals tubule-to-cyst transitions. a-b, Immunoblots of PC1 and PC2 in genome-modified PKD hPSCs or isogenic controls, from a representative experiment. Band intensity quantification of mature PC1 or PC2, normalized to β-actin, is shown (**a,** n=3 separate experiments, ± s.e.m., t(2.111)=12.64, *p*=0.0050; **b,** n=5 separate experiments, t(4.048)=10.4, *p*=0.0005). Full-length western blots are shown in Supplementary Information Fig. 7. **c,** Schematic of adherent cyst formation. Adherent cues (gradient rectangle) and stroma (pink cells) surround PKD tubules (green), which rarely form cysts. **d,** Phase-contrast images showing time courses of representative organoids in adherent cultures. Arrowheads indicate formation of the pre-cyst. Detachment is complete by day 35. Images are representative of > 20 cysts or tubules. Scale bar, 100 μm. **e,** Schematic of suspension cyst formation from a PKD organoid.

Supplementary Figure 2

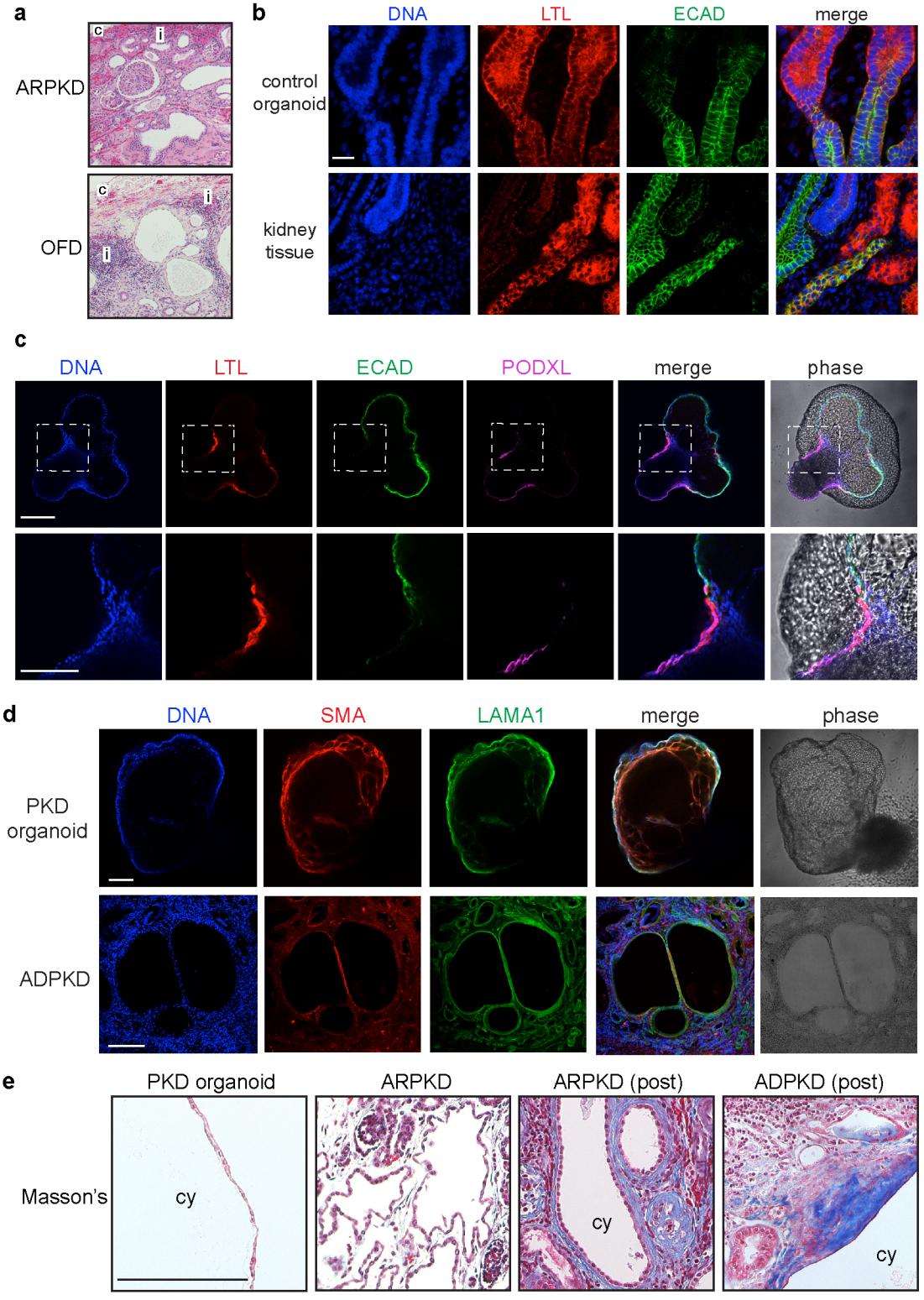

Supplementary Fig. 2. Organoid PKD cysts share features of PKD patient cysts. a, Paraffin sections dyed with hematoxylin and eosin from additional PKD patients. OFD, orofaciodigital syndrome. c, kidney capsule; i, inflammatory infiltrate. **b,** Confocal immunofluorescence showing ECAD and LTL in a representative PKD organoid cyst. Zoom is shown below for each channel. **d,** Confocal optical sections of samples shown in Fig. 2h, showing individual channels. **e,** Masson's trichrome staining in paraffin sections of PKD organoid cysts and human PKD kidneys. Blue staining indicates collagen deposits. Scale bars, 200 µm.

Supplementary Figure 3

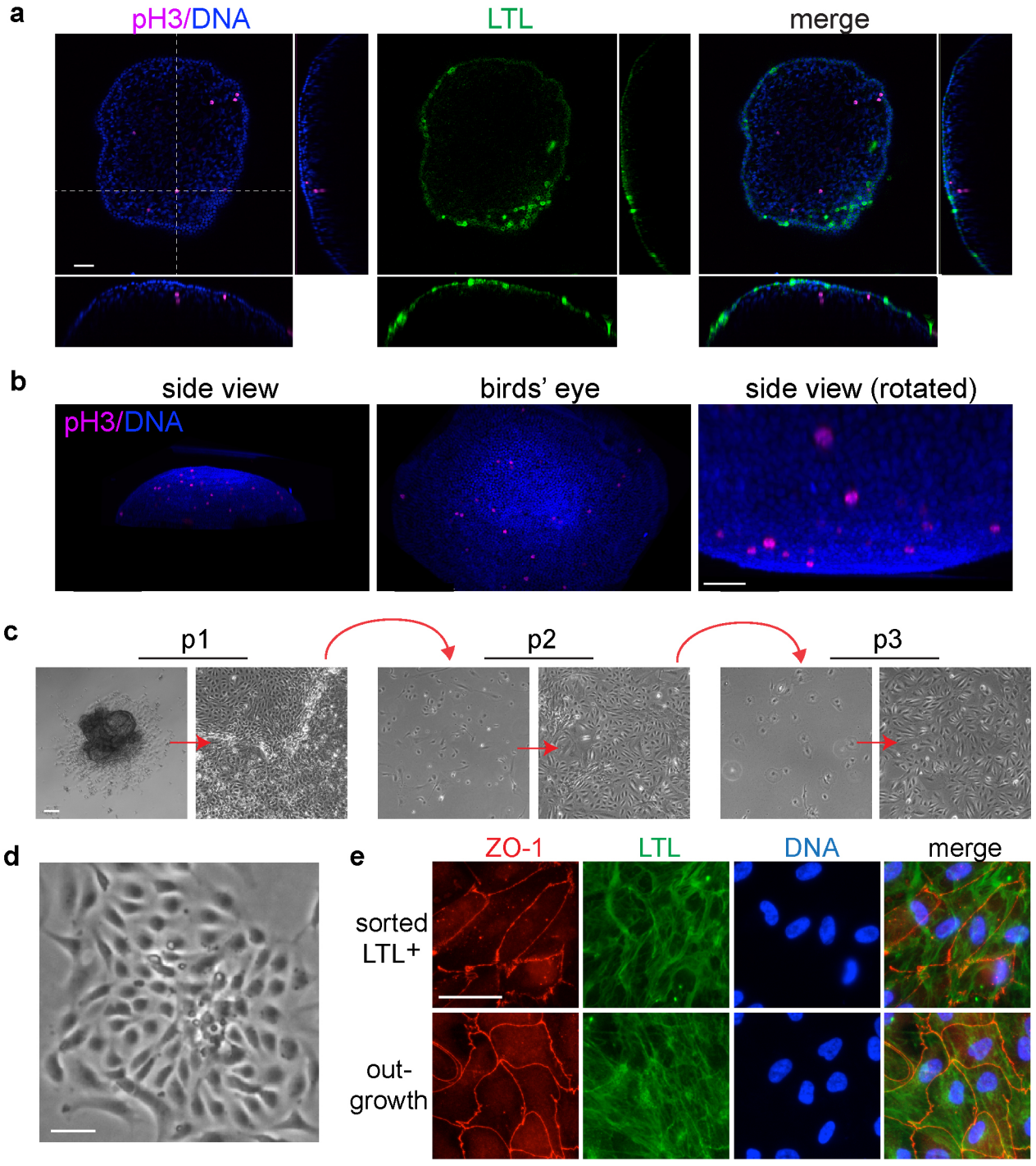

Supplementary Fig. 3. Cysts arise from proliferative KTECs. a, Confocal z-slice through a *PKD1*$^{-/-}$ cyst in suspension. Orthogonal planes are shown for the z planes indicated by dashed lines. **b,** Still frames from Movie 3 showing confocal volumetric reconstruction of this cyst from different perspectives. **c,** Phase contrast images of a kidney organoid explant (p1; red arrow) and two subsequent passages (p2, p3; red arrows). **d,** Phase contrast image of passage 1 KTECs showing cobblestone morphology. **e,** Comparative marker expression in outgrowth KTECs compared to LTL^{+} cells sorted from organoid cultures. Scale bars, 50 µm.

Supplementary Figure 4

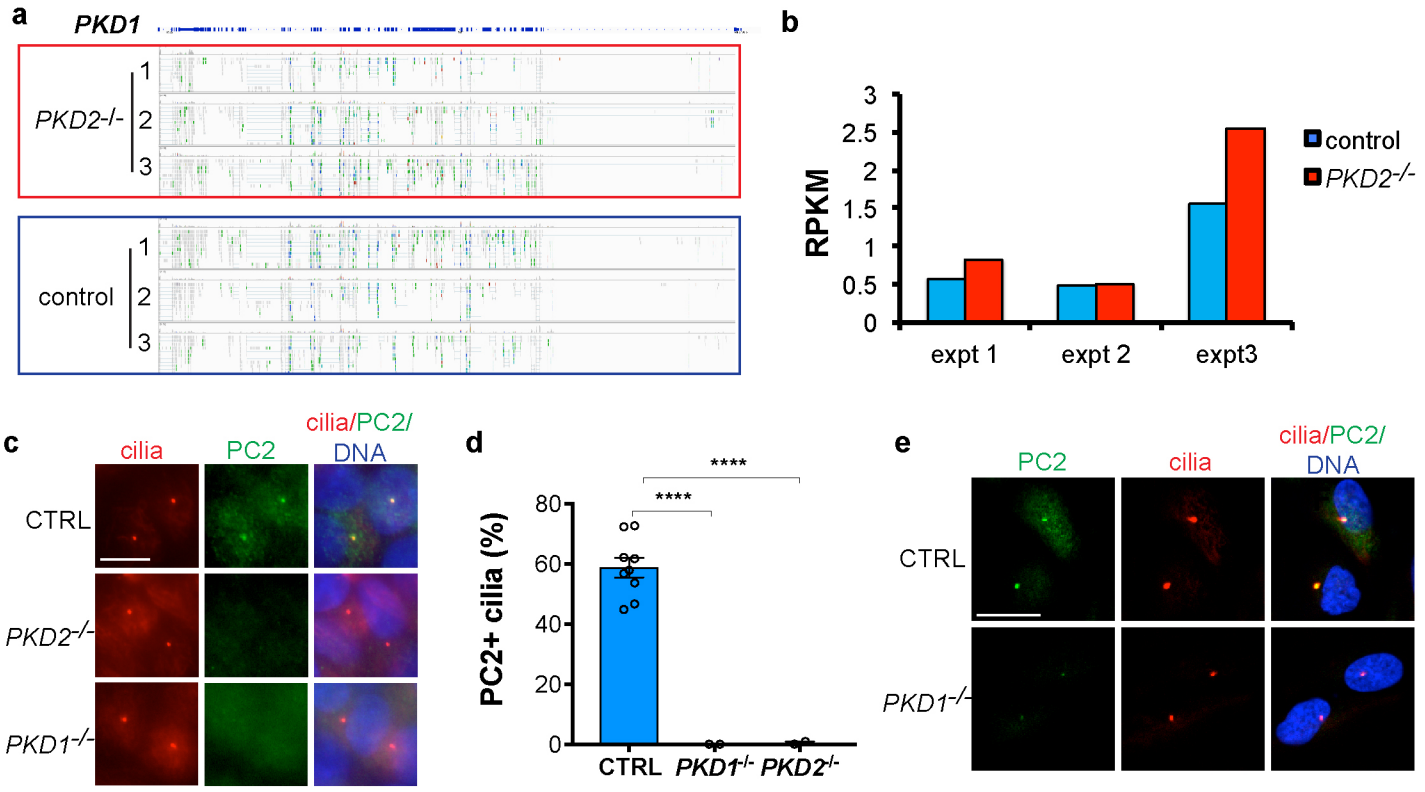

Supplementary Fig. 4. PC1 and PC2 interdependence is post-transcriptional. a, Representative RNA-Seq alignments for *PKD1* in hPSCs. Three independent experiments are shown for each genotype. Sequences are aligned to the reference sequence (blue diagram). **b,** Reads per kilobase million for *PKD1* in these three experiments (individual data points are shown). **c,** Representative immunofluorescence images of PC2 and cilia in undifferentiated *PKD1*$^{-/-}$ and *PKD2*$^{-/-}$ hPSCs, compared to isogenic controls. **d,** Quantification of ciliary PC2 in these lines (n = 9 ctrl and 2 each of *PKD1*$^{-/-}$ and *PKD2*$^{-/-}$ with ≥ 300 cilia counted per condition, ± s.e.m; ctrl vs. *PKD1*$^{-/-}$, t(8)=17.99, p=9.3564×10^{-8}; ctrl vs. *PKD2*$^{-/-}$, t(8.285)=17.68, p=7.1680×10^{-8}). **e,** Ciliary PC2 immunofluorescence in kidney organoid cells. Scale bars, 10 μm.

Supplementary Figure 5

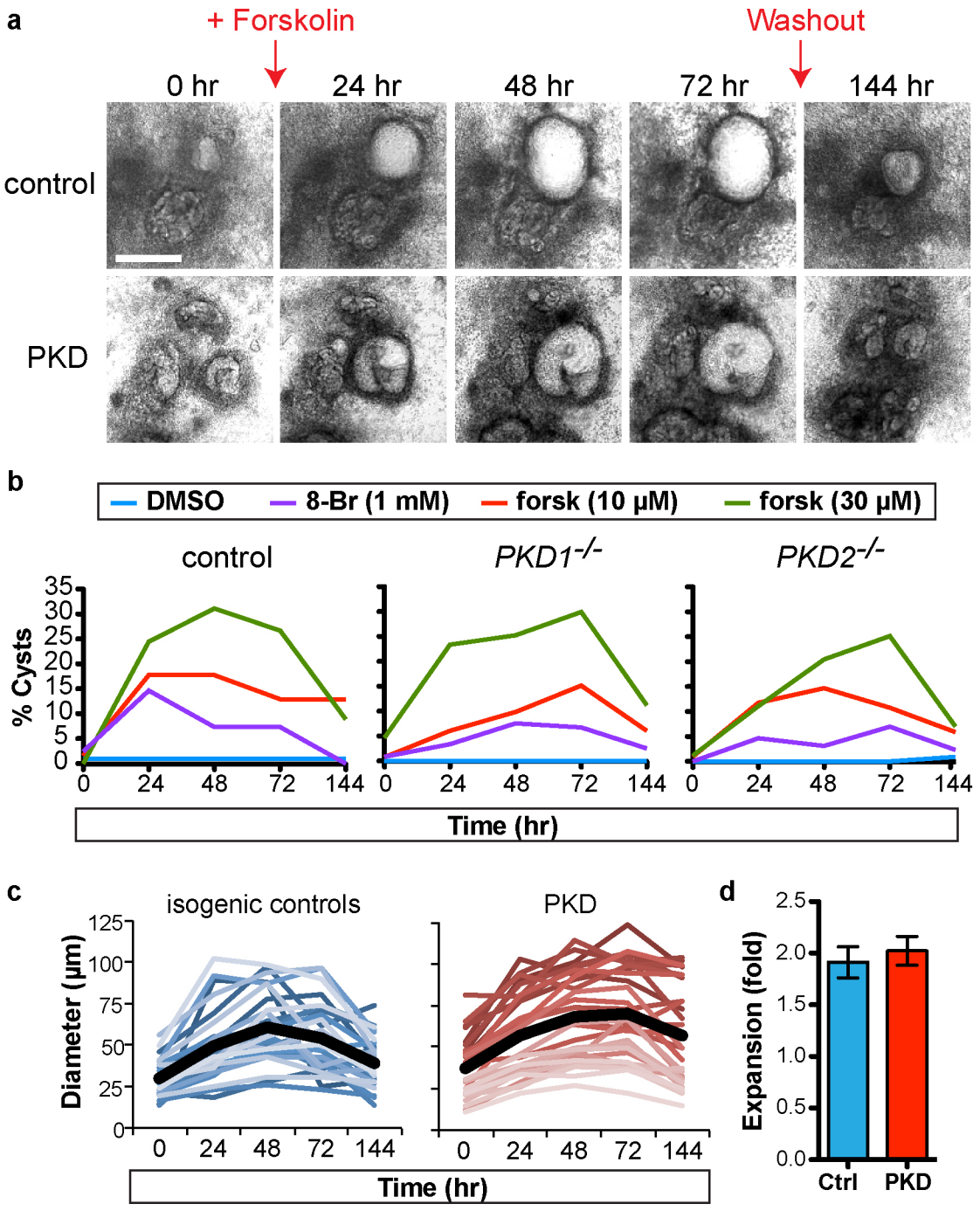

Supplementary Fig. 5. Cyclic AMP promotes cystogenesis in PKD organoids and isogenic controls. a, Representative stills from Movie 4 showing individual PKD organoids or isogenic controls treated for 72 hours with 30 μM forskolin, and subsequently returned to normal media for 72 hours (washout). **b,** Quantification of cyst formation in PKD or control organoids treated with forskolin, 8-Br-cAMP, or vehicle control in this experiment. Doses of 8-Br-cAMP < 1 mM did not produce cysts. **c,** Dynamics of cystic expansion in thirty PKD or control organoids after treatment with 30 μM forksolin. Each trace represents a single organoid, pooled from two experiments. Average of all traces is shown with bold black line. **d,** Average expansion at 72 hours (± s.e.m.). No significant difference is observed (p = 0.59). Scale bars, 100 μm.

Supplementary Figure 6

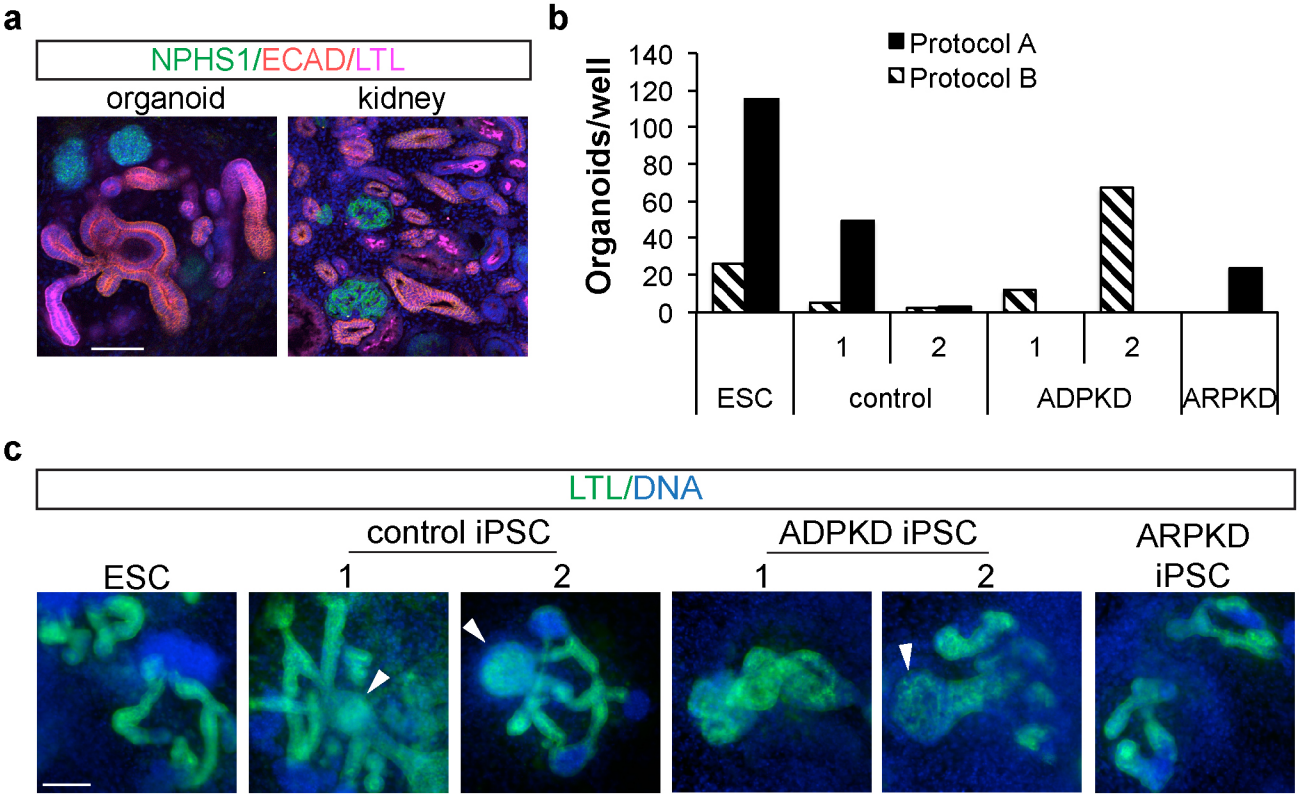

Supplementary Fig. 6. hPSCs from different patients exhibit variability in kidney organoid differentiation. a, Confocal immunofluorescence images showing iPSC-derived organoids and human kidney tissue, showing podocytes (NPHS1), distal tubules (ECAD), and proximal tubules (LTL). **b,** Quantification and **c,** representative images of kidney organoid differentiation in a cohort of one ESC line, two control iPSC lines, and three PKD iPSC lines. Two different differentiation protocols were attempted. Individual data points are shown. Arrowheads indicate cyst-like structures in these cultures. ARPKD, autosomal recessive PKD. Scale bars, 100 μm.

Supplementary Figure 7

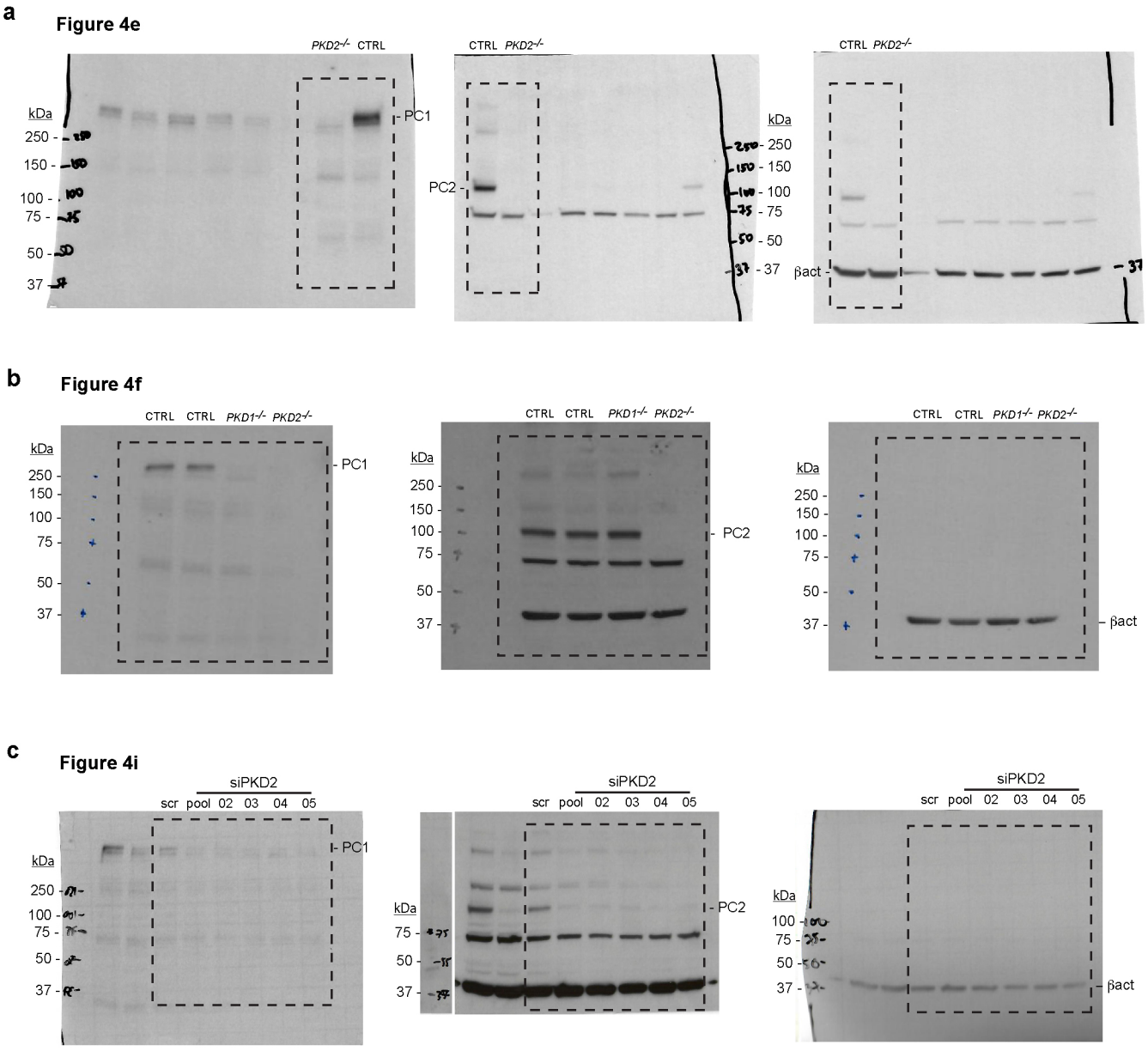

Supplementary Fig. 7. Full-length western blot images show PC1 depends on PC2. Original western blots for **a,** Figure 4e; **b,** Figure 4f; **c,** Figure 4i. Cropped areas used in Figure 4 are shown in bracket box. Prestained protein standards were visible on the blots and annotated manually by overlay of the film onto the nitrocellulose membrane. kDa sizes of the standards are indicated for clarity.